Catalytic properties of goethite prepared in the presence of Nb on oxidation reactions in water: Computational and experimental studies

ARTICLE *in* APPLIED CATALYSIS B ENVIRONMENTAL · SEPTEMBER 2008

Impact Factor: 7.44 · DOI: 10.1016/j.apcatb.2008.01.038

Available online at www.sciencedirect.com
ScienceDirect
Applied Catalysis B: Environmental 83 (2008) 169–176
APPLIED CATALYSIS B: ENVIRONMENTAL
www.elsevier.com/locate/apcatb

Catalytic properties of goethite prepared in the presence of Nb on oxidation reactions in water: Computational and experimental studies

Luiz C.A. Oliveira [a,*], Teodorico C. Ramalho [a], Eugênio F. Souza [a], Maraísa Gonçalves [a], Diana Q.L. Oliveira [b], Márcio C. Pereira [b], José D. Fabris [b]

[a] *Departamento de Química, Universidade Federal de Lavras (UFLA), Caixa Postal 37, CEP 37200-000 Lavras, Minas Gerais, Brazil*
[b] *Departamento de Química, Universidade Federal de Minas Gerais (UFMG), Campus Pampulha, CEP 31270-901 Belo Horizonte, Minas Gerais, Brazil*

Received 9 March 2007; received in revised form 25 January 2008; accepted 30 January 2008
Available online 20 February 2008

Abstract

Nb-substituted goethites have been prepared and characterized by Mössbauer spectroscopy, XRD, FTIR and BET surface area measurements. The doublet formation in Mössbauer spectra and the decreasing of the crystallinity shown in XRD analyses indicated that the Fe domain size is small, which may be the result of either Fe^{3+} substitution for Nb^{5+} in the goethite structure or simply the formation of small particle-size goethite when Nb is present. FTIR analyses showed shifts and broadening of the bands as result of the incorporation of Nb^{5+} ions into the α-FeOOH structure. The insertion of Nb in the goethite structure caused a significant increase in the BET surface area of the material. The prepared materials were investigated for the H_2O_2 decomposition and the Fenton reaction in the oxidation of methylene blue dye. It was observed that the introduction of Nb during the synthesis of goethite produced a strong increase in the activity for the dye contaminant oxidation by H_2O_2. Theoretical quantum DFT calculations were carried out in order to understand the degradation mechanism for methylene blue with goethites.

Keywords: Goethite; Niobium; DFT; Fenton reaction

1. Introduction

Reactions involving hydrogen peroxide decomposition catalyzed by iron oxides, to generate radical *OH, have received special attention due to the advantages in relation to the classic homogeneous process involving iron soluble salts (Fenton reaction) [1]. These advantages are: (i) it is a heterogeneous system, facilitating all the operations in the treatment of the effluent; (ii) it operates in neutral pH, thus avoiding the need for acidification stages (pH 3) or further neutralization, thus preventing the generation of sludge; and (iii) the system can be recycled/regenerated by reducing surface Fe^{3+} species. Several recent studies have investigated different iron containing solids for the Fenton reaction, such as Fe_2O_3 and $Fe_2Si_4O_{10}(OH)_2$ [2,3], goethite [4–6], Fe(II) supported on zeolite, Al_2O_3 and SiO_2 [7,8] and Fe^0/Al_2O_3 [9]. It has been observed that depending on the conditions employed, these materials can promote the oxidation of different organic compounds, such as, aromatic and aliphatic acids, phenols, aromatic hydrocarbons, chloro compounds and textile dyes with hydrogen peroxide. However, many of these systems showed low activity or strong iron leaching due to low pH, which resulted in the classical homogeneous Fenton mechanism.

In the present work, the reactivity of the heterogeneous Fenton system over goethite was studied. Methylene blue dye was used as a probe contaminant. We carried out experiments to investigate the effect of niobium contents in goethite on the UV/vis and ESI-MS monitored degradation of dye in the presence of H_2O_2.

Targeting a better understanding of the role of niobium in the H_2O_2 decomposition, theoretical calculations were carried out at the Density Functional Theory (DFT) level.

2. Experimental

2.1. Goethite synthesis and characterization

All chemicals were high purity grade and were used as purchased. Goehite α-FeOOH was prepared from $FeCl_3{\cdot}6H_2O$,

* Corresponding author.
E-mail address: luizoliveira@ufla.br (L.C.A. Oliveira).

0926-3373/$ – see front matter © 2008 Elsevier B.V. All rights reserved.
doi:10.1016/j.apcatb.2008.01.038

NaOH and by co-precipitation followed by thermal treatment at 60 °C (72 h) [10]. The substituted goethites were prepared as described above with the addition of 4 (Nb4), 7 (Nb7) and 11% (Nb11) in mass of ammonium niobium oxalate (general formula $NH_4[NbO(C_2O_4)_2(H_2O)](H_2O)_n$ supplied by CBMM (Companhia Brasileira de Metalurgia e Mineração, Araxá-MG).

The surface area was determined by the BET method using N_2 adsorption/desorption in an Autosorb 1 Quantachrome instrument. Transmission Mössbauer spectroscopy experiments were carried out in a CMTE spectrometer model MA250 with a ^{57}Co/Rh source at room temperature using αFe as reference. The powder XRD data were obtained in a Rigaku model Geigerflex using Cu Kα radiation scanning from 2 to 75° at a scan rate of 4° min^{-1}. A scanning electron microscope (SEM) manufactured by JEOL Ltd., was used. SEM was coupled with EDS/INCA 350 (energy dispersive X-ray analyzer) manufactured by Oxford Instruments. DSC (RIGAKU MOD 8065 D1) analysis was operated in an air atmosphere with a heating rate of 10 °C min^{-1}.

2.2. Reactions

The hydrogen peroxide (Synth) decomposition study was carried out with 5 mL of 2.9 mol L^{-1} H_2O_2 and 10 mg of catalyst by measuring the formation of gaseous O_2 in a volumetric glass system. The oxidation of 50 mg L^{-1} methylene blue dye with H_2O_2 (0.3 mol L^{-1}) at pH 6.0 (natural pH of the H_2O_2 solution) was carried out with a total volume of 10 mL and 10 mg of the oxide catalyst. The reactions were monitored by UV–vis measurements (Shimadzu-UV-1601 PC). All the reactions were carried out under magnetic stirring in a recirculating temperature controlled bath kept at 25 ± 1 °C.

2.3. Studies by ESI-MS

In an attempt to identify the intermediate formation, the methylene blue decomposition was also monitored with the positive ion mode ESI-MS of an Agilent MS-ion trap mass spectrometer. The reaction samples were analyzed by introducing aliquots into the ESI source with a syringe pump at a flow rate of 5 mL min^{-1}. The spectra were obtained as an average of 50 scans of 0.2 s. Typical ESI conditions were as follows: heated capillary temperature of 1508 °C; sheath gas (N_2) at a flow rate of 20 U (4 L min^{-1}); spray voltage of 4 kV; capillary voltage of 25 V; tube lens offset voltage of 25 V.

2.4. Computational methods

The calculations were carried out with the package Gaussian98 [11]. All the transition states, intermediates and precursors involved were calculated. Each conformer was fully optimized by DFT [12]. Density Functional Theory (DFT) methods have been increasingly applied to the study of reaction mechanisms. This approach is interesting because it includes the effect of electronic correlations and allows for the calculation of larger systems [13,14]. Nowadays, that is a well-established technique applied to numerous cases [14–17]. The energy profile at selected DFT geometries along the reaction pathway has been computed at B3LYP level of theory using the 6-31+G (d,p) basis set. The DFT calculations were applied with the functional correlation of Lee, Yang and Parr (LYP), which includes both local and non-local terms [13,14], and Becke's 1988 function, which includes Slater exchange along with corrections involving the gradient of electronic density (B3LYP). For all the different calculation methods, the algorithms conjugate gradient and quasi-Newton-Raphson were used for the geometry optimization until a gradient of 10^{-9} atomic units was obtained. The final geometries were obtained with DFT using the density functional B3LYP using the basis set 6-311+G** [13,14]. This computational procedure has been employed previously on similar systems with success [15,16]. Furthermore, after each optimization the nature of each stationary point was established by calculating and diagonalizing the Hessian matrix (force constant matrix). The unique imaginary frequency associated with the transition vector (TV) [17], i.e., the eigenvector associated with the unique negative eigenvalue of the force constant matrix, has been characterized.

3. Results and discussion

3.1. Characterization

Elemental analysis by EDS confirmed that samples Nb4 and Nb11 contained 4 and 11% niobium, respectively. The powder XRD patterns of the pure goethite and Nb4 samples (not showed here) indicate the presence of a hexagonal crystalline phase (d = 0.497, 0.418, 0.336, 0.269, 0.244, 0.225 and 0.172 nm) relative to goethite. The broadening of the reflections of the Nb4 sample compared to reflections observed in the pure goethite sample indicates that niobium induces a decrease in particle size, but falls short of proving that isomorphic substitution of Fe^{3+} by Nb^{5+} has occurred because the ionic radius of both Fe^{3+} and Nb^{5+} is 64 pm and thus no change in lattice parameter can be observed. The increase in non-crystalline materials in the XRD patterns obtained for the Nb7 and Nb11 samples revealed that Nb induced a loss of crystallinity in the goethite which was proportional to the Nb content.

The Mössbauer parameters (Table 1) for the materials were consistent with a mixture of pure and substituted goethite particles. Pure, well crystallized goethite gives a magnetically ordered Mossbauer spectrum (sextet) at room temperature. As non-magnetic cations (e.g., Nb) substitute for Fe in the goethite structure, the magnetic domain size decreases and the magnetic order disappears, causing the sextet to collapse into a doublet. In agreement with XRD, the Mössbauer spectra for the Nb4, Nb7 and Nb11 samples therefore revealed that niobium substitution lead to a decrease in the crystallinity and/or particle size and crystalline perfection as evidenced by the appearance of the observed central doublets (Fig. 1). The quadrupole shift also decreased, indicating that the increased niobium content distorted the crystalline structure of the

Table 1
Fitted room temperature Mössbauer parameters for goethites (δ = isomer shift relative to αFe; ε = quadrupole shift, Δ = quadrupole splitting; B_{hf} = hyperfine field and RA = relative sub-spectral area)

Sample	δ (mm s^{-1})	ε, Δ (mm s^{-1})	B_{hf} (T)	RA (%)	Phase
Pure goethite	0.377(3)	−0.250(6)	36.5(1)	88.5(2)	Gt
	0.371(7)	0.69(3)		11.5(2)	$^{VI}Fe^{3+}$
Nb4	0.36(1)	−0.21(2)	35.98(1)	22.3(2)	Gt
	0.369(9)	0.70(3)		77.7(2)	$^{VI}Fe^{3+}$
Nb7	0.41(3)	−0.18	36.11(6)	7.8(2)	Gt
	0.354(2)	0.707(3)		92.2(2)	$^{VI}Fe^{3+}$
Nb11					
	0.346(2)	0.713(3)		100.0(5)	$^{VI}Fe^{3+}$

goethite due to the substitution of Fe by Nb. Moreover, the isomer shift of the doublets decreased with an increase of Nb content. This fact is evidence that isomorphic substitution of Fe by Nb is occurring in the goethite. Nb has a smaller electronegativity than Fe, which causes a decrease in the isomer shift. In Nb11 sample the magnetic domain size is so small that no magnetic order is observed. Some studies [18,19] asserted that the disappearance of the sextet in the Mössbauer spectra of goethite in favor of a doublet is evidence of oxygen vacancy sites in the goethite structure. Because the presence of niobium during the preparation of goethite produces a structure characterized by this same collapse of the sextet into a doublet, oxygen vacancy sites may be increasingly present in samples Nb7 and Nb11, which suggests the incorporation of Nb into the goethite structure. Morales et al. [20], Schwertmann et al. [21] and Krehula et al. [19,22] concluded that the main effect of doping with several cations, such as Ni, Cr, Mn, and Ga, was a reduced goethite crystallite size.

The FTIR spectrum of pure goethite (Fig. 2a) contains an intense band at 3150 cm^{-1}, due to bulk hydroxyl stretching, and important diagnostic O–H bending bands at about 890 (Fe–OH) and 793 (Fe–OH) cm^{-1}, which vibrate in and out of the plane, respectively [8], and at 635 cm^{-1} (Fe–O stretching). FTIR spectra of doped goethite showed similar features to the pure goethite, except the sample with high Niobium content (sample

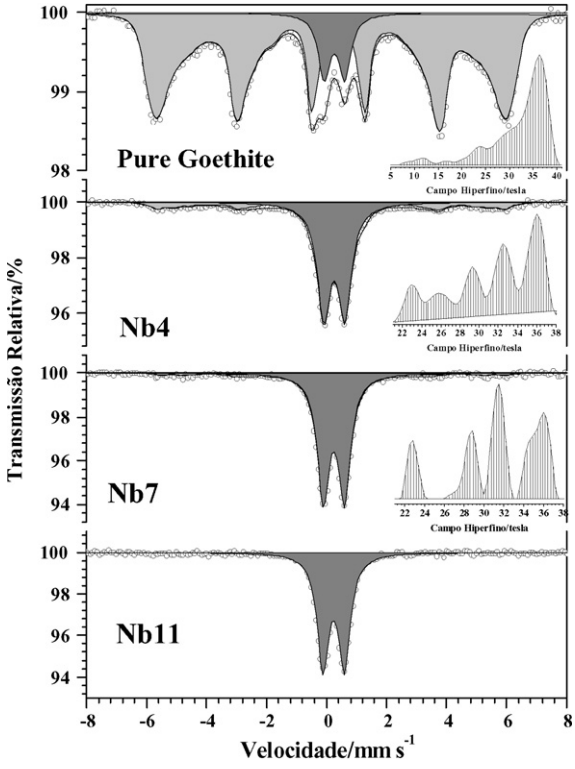

Fig. 1. Mössbauer spectra of the goethites at room temperature.

Nb11) exhibited noticeable spectral differences from pure goethite. The Fe–O stretching band was broadened and shifted to 609 cm^{-1} and the O–H bending band at 890 cm^{-1} shifted to 858 cm^{-1}, which is consistent with Nb being incorporated into the goethite structure [22]. Stiers and Schwertmann [23] also reported shifts in the O–H bending band at 888 cm^{-1} with increased substitution of Mn^{3+} or Al^{3+} for Fe^{3+} in goethite.

DSC analyses revealed that increasing the Nb content of the sample increased the temperature at which the phase transition of goethite to hematite occurred (Fig. 2b), shifting from approximately 218 °C for pure goethite in air to 251 °C and 271 °C for samples Nb7 and Nb11 in air, respectively. For synthetic and natural goethites the temperature of this

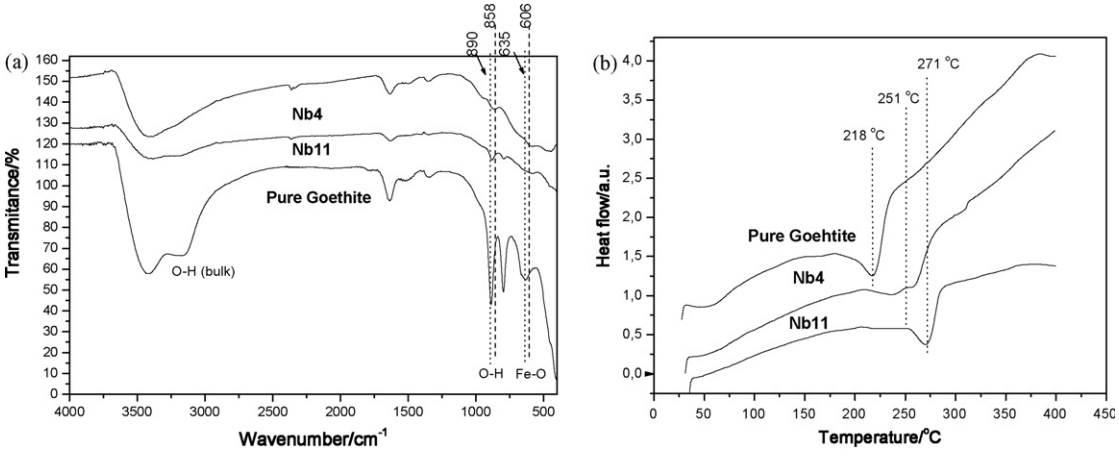

Fig. 2. FTIR (a) and DSC (b) analyses of the pure goethite, Nb4 and Nb11.

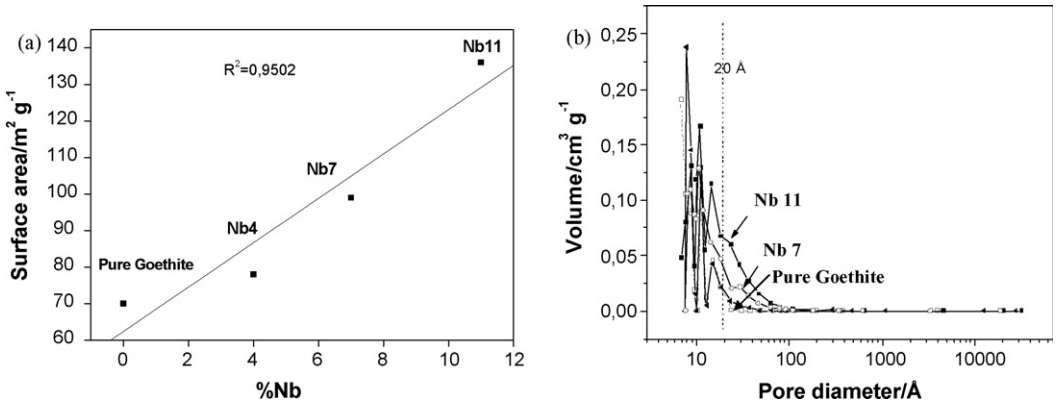

Fig. 3. Variation of specific surface area with Nb presence (a) BJH pore size distribution (b) of the goethites.

endothermic peak is well known to increase with increasing crystallite size [24–25]; but, as the XRD and Mössbauer data showed, increasing the Nb content actually decreases the crystallinity of the goethite [10]. This phenomenon was further confirmed by N_2 adsorption–desorption analysis, which found that the BET specific surface areas of pure goethite, Nb4, Nb7, and Nb11 (Fig. 3a) increased in the order 70, 78, 99, and 136 $m^2\ g^{-1}$, respectively. The crystallinity and crystallite size should vary inversely with these values, especially in the mesoporous region. The observed increase in BET surface area is likely also related to an increase in the pore diameter. The pore-size distributions were determined with the Barrett–Joyner–Halenda (BJH) pore size distribution for these samples (Fig. 3b) clearly showed that the presence of Nb gradually produced materials with greater pore diameters.

Scanning electron micrographs of the samples revealed that Nb substitution changes the morphology from a smooth surface in the pure goethite (Fig. 4a) to rough surface in samples Nb4 and Nb11 (Figs. 4c and e).

3.2. H_2O_2 decomposition

The catalytic activity of the goethites was studied using two reactions: (i) H_2O_2 decomposition to O_2 ($H_2O_2 \rightarrow H_2O + 1/2O_2$); and (ii) oxidation of the model contaminant methylene blue dye with H_2O_2 in aqueous medium. The decomposition of H_2O_2 in the presence of the different goethite samples approximately followed pseudo zero-order kinetics, as indicated by the nearly linear plots obtained between H_2O_2 concentration and time of reaction (Fig. 5a). Ferraz et al. [26] proposed that in the presence of other iron phases the decomposition mechanism involves radical formation, such as *OH or *OOH [25], but this apparently is not true in the present case, at least within the first 60 min, because the addition of phenol, a radical scavenger that would react with radical intermediates, had no inhibitory effect on the H_2O_2 decomposition rate in the presence of sample Nb11 (Fig. 5b). The same result was also observed when hydroquinone or ascorbic acid was added (Fig. 5b). Perhaps this is because of a competitive process involving the organic substrate and the active surface, such as proposed by Costa et al. [27]. In this scenario, oxygen vacancies $[]_{surf}$ at the oxide surface react with H_2O_2 to produce O_2 (Eq. (1) and (2)). This mechanism was first proposed, however, for oxides such as perovskite [27] and is believed to be uncommon in the iron oxides.

$$[] + H_2O_2 \rightarrow H_2O + [O_{ads}] \quad (1)$$

$$2[O_{ads}] \rightarrow O_2 \quad (2)$$

3.3. Methylene blue dye oxidation

The oxidation of methylene blue by H_2O_2 in the presence of goethite may be represented by Eq. (3):

$$\text{methyleneblue} \rightarrow \text{partiallyoxidizedintermediates} \rightarrow \rightarrow \rightarrow CO_2 + H_2O \quad (3)$$

and is monitored by UV–vis absorption at 663 nm. In the control experiment where goethite was absent, no significant discoloration was observed (Fig. 6) even after 120 min reaction. In the presence of pure goethite, a low activity of methylene blue dye oxidation was observed with only 15% color reduction after 120 min. On the other hand, in the presence of Nb-substituted goethite Nb11, catalytic discoloration of up to 85% was observed after 120 min.

3.4. Identification of intermediates via On-line ESI-MS monitoring

Reaction intermediates from oxidation of methylene blue dye in the presence of Nb11 were identified in real time using ESI-MS (Fig. 7). As expected, at zero reaction time (Fig. 7a), with the ESI-MS operating in the positive ion mode, the presence of only a single cation ($m/z = 284$) in aqueous solution was observed. However, after 60 min of reaction (Fig. 7b) a new and relatively intense signal with $m/z = 270$ was also clearly detected. After reaction time of 180 min (Fig. 7c) the signals with $m/z = 105, 129, 187, 227$, and 270 were detected. Based on the detection of these m/z signals a simple reaction scheme (Fig. 8) with intermediates **I–V.3** can be proposed for the oxidation of methylene blue dye by the Nb11 catalyst.

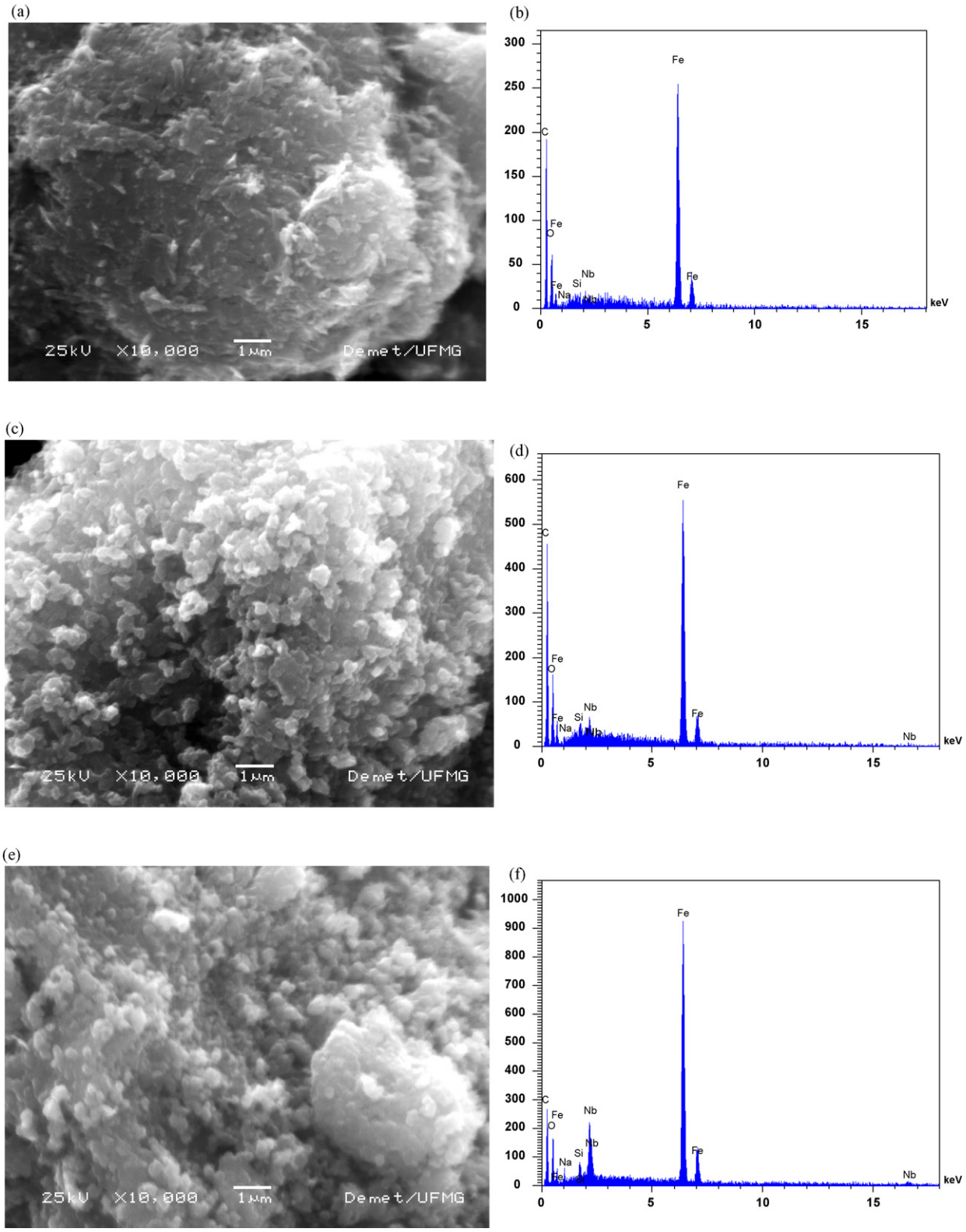

Fig. 4. SEM and EDS analyses of the goethites with niobium.

3.5. Theoretical results

According to the conventional mechanism for H_2O_2 decomposition in a Fenton reaction, the reaction may be initiated by an iron active site on the surface of the composite, at which the H_2O_2 produces a *OH; or, by a process that involves the peroxide itself which transfers an electron to an oxidizing site yielding a *OOH species [28]. According to the latter mechanism, the fragmentation pathway would be similar to the one described in a previous paper [25]; but, as shown in Fig. 7,

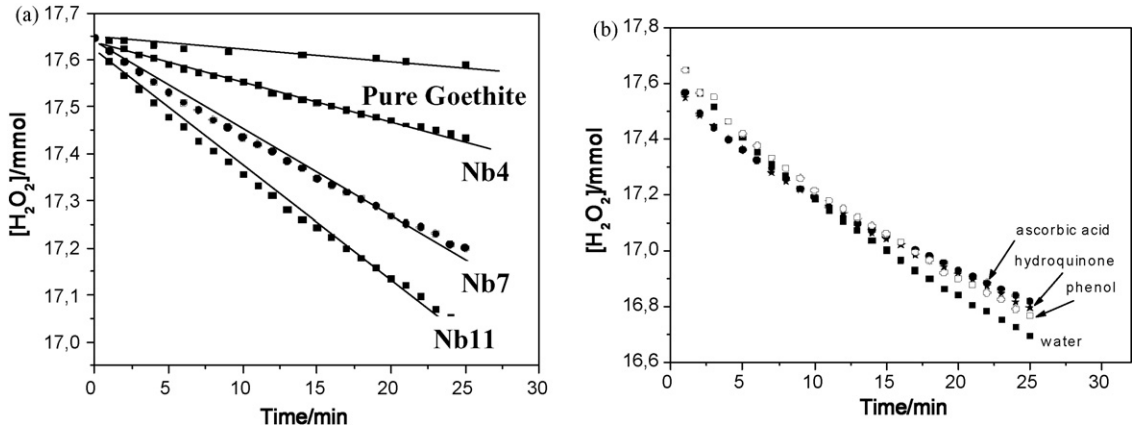

Fig. 5. The H_2O_2 decomposition in water (a) and with organic compounds (b) in the presence of the different goehites.

the fragmentation path for methylene blue dye observed in the present study was considerably different. Instead, previously uninvestigated degradation intermediates were observed. This strongly suggests a new reaction mechanism in which the reaction is initiated by neither of the conventional ways. The mechanism for the Nb-goethite catalyst could, therefore, involve oxygen vacancies at the goethite surface, which differs from the heterogeneous Fenton reaction described in the literature for iron phases [19].

In order to shed more light on this alternative reaction mechanism for Nb-substituted goethites, Gibbs free energy calculations were performed using the *Gaussian98* software to determine the stability of intermediates [11]. All discussions concerning the energy differences and the energy barriers refer to the Gibbs term, corrected for the zero point energy at 298.15 K. Results from the theoretical model agreed well with the experimental geometry for the methylene blue molecule [23]. After 60 min of reaction, the most intense fragment observed in mass spectra corresponded to $m/z = 270$ (Fig. 7), which is associated with the loss of a methyl group.

Further insight was obtained by performing *ab initio* calculations of thermodynamic stability (Table 2), which identified an energy barrier of 24 kcal mol^{-1} for the formation of intermediate product **II**. This energy is considerably lower than that involved in the hydroxylation of the aromatic ring [25]. As expected, the participation of the oxygen vacancies on the oxide surface in the oxidation reaction resulted in chemical species less reactive than the *OH radical in solution. The formation of **II** was followed by additional loss of a –N(CH3) group, resulting in intermediate product **III** ($m/z = 227$) with an energy barrier of +83.25 kcal mol^{-1} (Table 2, Fig. 8). The loss of the –NH(CH3) group can produce a neutral fragment (**IV**), $m/z = 198$, from **III** to **IV**, with an energy barrier of +58.67 kcal mol^{-1}. Due to its total charge, this fragment is undetected experimentally; however, we believe that **IV** could be a key intermediate for formation of an important fragment observed at $m/z = 187$ (Fig. 7). This fragment is associated with

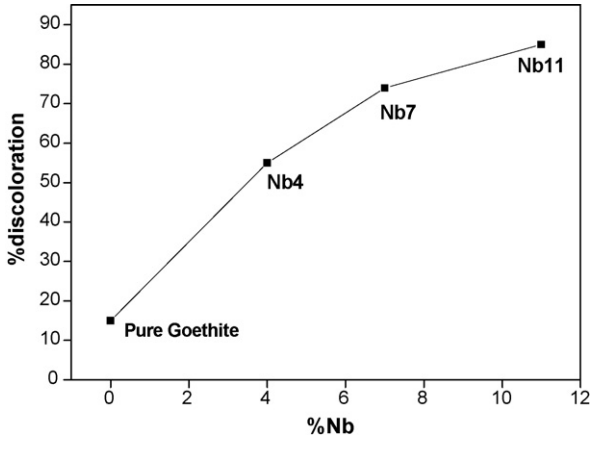

Fig. 6. Discoloration measurements using the dye methylene blue as probe molecule in the presence of goethites with niobium.

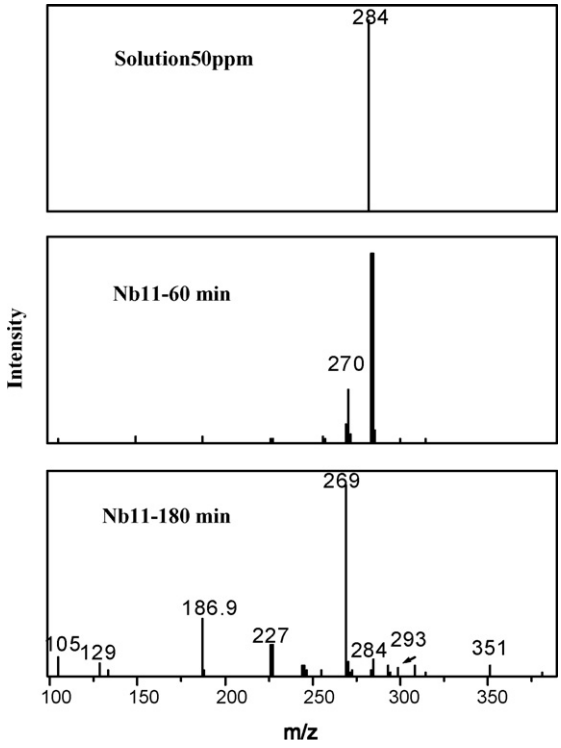

Fig. 7. ESI mass spectra in the positive ion mode for monitoring the oxidation of methylene blue dye in water by the goehites and H_2O_2 system at different reactions times.

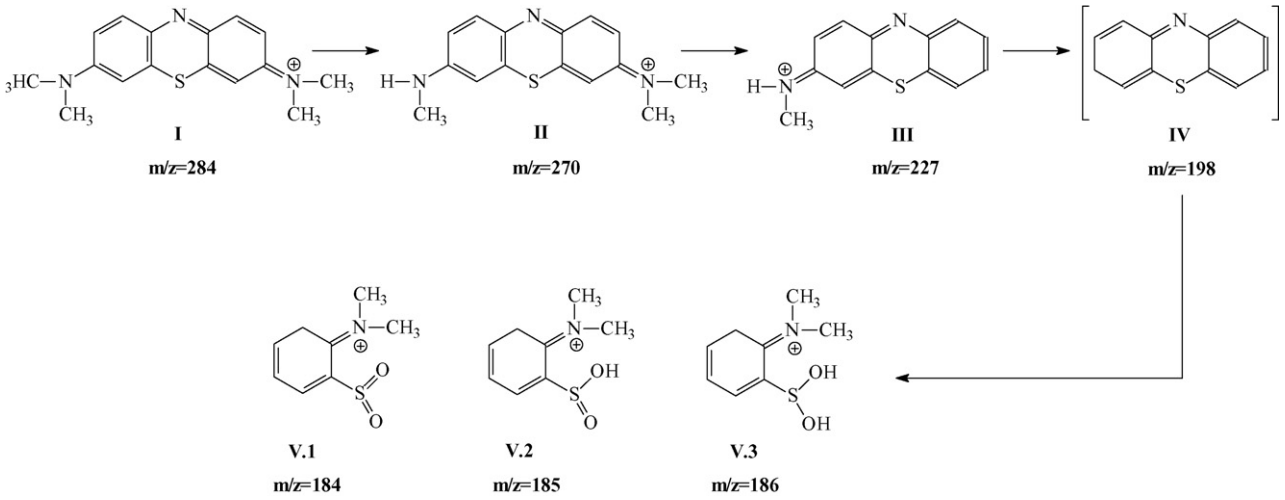

Fig. 8. Scheme with intermediates proposed for the oxidation of methylene blue dye ($m/z = 284$) by goethites and H_2O_2 system.

possible structures **V.1–3** (Fig. 8). According to data listed in Table 2, energy barriers of 1.29, 0.84, and 0.46 kcal mol^{-1} may be attributed to the intermediates **V.1**, **V.2** and **V.3**, respectively. This means that the intermediate **V.3** is more stable than other alternatives and that **IV** would be a key intermediate that points out the rapid and high probability of formation of **V.3**. Again, in this case no hydroxylation on the aromatic ring occurs, in contrast to a Fenton-like mechanism [25].

At the second step of the transformation (180 min of reaction), the magnitude of the signals $m/z = 105$, 129, and 351 are significant (Fig. 7). These signals have already been well characterized both experimentally and theoretically as a result of hydroxylation of aromatic ring through a Fenton-like mechanism, which was followed by formation of hydroquinone-like intermediates generated by *OH attack. This is an unstable, but key intermediate which points out the facility with which the chemical bonds of the aromatic ring rupture. This could then account for the formation of the signals $m/z = 105$ and 129. Thus, our results indicate that two competing mechanisms could occur: (i) reaction at the oxygen vacancy sites in Nb-substituted goethites, yielding the intense fragments $m/z = 270$, 227, and 187 (Fig. 7), which are associated with intermediates **II**, **III**, and **IV**, respectively (Fig. 8); and (ii) a Fenton mechanism resulting in fragments $m/z = 105$, 129, and 351. The fist step of the transformation (60 min of reaction) would occur preferentially via mechanism (i), whereas both mechanisms (i) and (ii) could occur simultaneously at the second step (180 min) of the transformation.

Table 2
Gibbs free energy of the reaction intermediates using B3LYP/6-311+G**

Intermediate	ΔG (kcal mol^{-1})
I	0.00
II	+24.59
III	+83.25
IV	+58.67
V.1	+1.29
V.2	+0.84
V.3	+0.46

As discussed above and as noted previously [25], the degradation of methylene blue via a Fenton-like mechanism exhibits an induction period at the beginning of the reaction, which suggests that some degradation intermediates play an important role in promoting the Fenton reaction. The presence of *OH in the reaction medium, nevertheless, probably invokes the oxidation of I, which in turn can generate, for instance, the stable species with $m/z = 105$, 129, and 351. In line with this observation, at the first moment of reaction the hydrogen peroxide decomposition could take place via mechanisms (i) generating the fragments $m/z = 270$, 227, and 187. These results are, therefore, evidence that the oxidation reaction of methylene blue in water with goethites likely occurs through both of the competitive mechanisms (i) and (ii), but further and more accurate theoretical calculations are needed to verify the vacancy sites mechanism (i).

Until now, no other theoretical study has investigated the degradation of methylene blue via a heterogeneously catalyzed Fenton reaction. One should keep in mind, however, that the mechanisms for hydrogen peroxide decomposition cannot be completely understood from these observations. Several electron transfer processes are thought to take place during that reaction.

4. Conclusion

The hypothesis that Nb substitution in goethite creates surface oxygen vacancies in the Nb-goethite is supported by Mössbauer spectra, by hydrogen peroxide decomposition behavior in the presence of radical scavengers, and by the catalytic oxidation of organic dye as shown by ESI-MS. Understanding the mechanisms for catalysis is relevant to the formulation of novel, efficient, and cost-effective processes for the remediation of organic contaminants in wastewaters. The theoretical results presented herein suggest that two competitive mechanisms could occur in Nb-substituted goethites; one involving surface oxygen vacancies in Nb-substituted goethite and the other following a Fenton-like process.

Acknowledgments

Work supported by CNPq and FAPEMIG (Brazil). Authors are indebted to prof. Dr. C. A. Taft (CBPF) for the computation facilities, Patricia-Patterson for SEM-EDS analyses, Profa. Irene Yoshida (UFMG) for DSC analyses and CAPQ (Ufla).

References

[1] R.C.C. Costa, M.F.F. Lelis, L.C.A. Oliveira, J.D. Fabris, J.D. Ardisson, R.R.V.A. Rios, C.N. Silva, R.M. Lago, J. Hazard. Mater. 129 (2006) 171.
[2] R.L. Valentine, H.C. Ann Wang, J. Environ. Eng. 124 (1998) 31–38.
[3] J. He, X. Tao, W. Ma, W. Jincai, Chem. Lett. (2002) 66–87.
[4] M. Lu, C. Chun, N. Jong, H.H. Huang, Chemosphere 46 (2002) 131–136.
[5] R. Andreozzi, A. D'Apuzzo, R. Marotta, Water Res. 36 (2002) 4691–4698.
[6] S.R. Kunel, B. Neppolian, H. Choi, J.W. Yang, Soil Sediment Contam. 12 (2003) 101–117.
[7] G. Ceti, P. Perathoner, T. Torre, M.G. Verduna, Catal. Today 55 (2000) 61–69.
[8] N. Al-Hayek, M. Dore, Water Res. 24 (1990) 973–982.
[9] R.J. Watts, M.D. Udell, S.H. Kong, Environ. Eng. Sci. 16 (1999) 93–103.
[10] R.M. Cornell, U. Schwertmann, The Iron Oxides, 2nd ed., Weinheim-VHC, New York, 2003.
[11] Gaussian 98, Revision A.9, M.J. Frisch, G.W. Trucks, H.B. Schlegel, G.E. Scuseria, M.A. Robb, J.R. Cheeseman, J.A. Montgomery Jr., T. Vreven, K.N. Kudin, J.C. Burant, J.M. Millam, S.S. Iyengar, J. Tomasi, V. Barone, B. Mennucci, M. Cossi, G. Scalmani, N. Rega, G.A. Petersson, H. Nakatsuji, M. Hada, M. Ehara, K. Toyota, R. Fukuda, J. Hasegawa, M. Ishida, T. Nakajima, Y. Honda, O. Kitao, H. Nakai, M. Klene, X. Li, J.E. Knox, H.P. Hratchian, J.B. Cross, V. Bakken, C. Adamo, J. Jaramillo, R. Gomperts, R.E. Stratmann, O. Yazyev, A.J. Austin, R. Cammi, C. Pomelli, J.W. Ochterski, P.Y. Ayala, K. Morokuma, G.A. Voth, P. Salvador, J.J. Dannenberg, V.G. Zakrzewski, S. Dapprich, A.D. Daniels, M.C. Strain, O. Farkas, D.K. Malick, A.D. Rabuck, K. Raghavachari, J.B. Foresman, J.V. Ortiz, Q. Cui, A.G. Baboul, S. Clifford, J. Cioslowski, B.B. Stefanov, G. Liu, A. Liashenko, P. Piskorz, I. Komaromi, R.L. Martin, D.J. Fox, T. Keith, M.A. Al- Laham, C.Y. Peng, A. Nanayakkara, M. Challacombe, P.M.W. Gill, B. Johnson, W. Chen, M.W.Wong, C. Gonzalez, J.A. Pople, Gaussian Inc., Wallingford CT, 1998.
[12] H.G. Li, G.K. Kim, C.K. Kim, S. Rhee, I. Lee, J. Am. Chem. Soc. 123 (2001) 2326.
[13] A.D. Becke, J. Chem. Phys. 98 (1993) 5648.
[14] S. El-Taher, R.H. Hilal, Int. J. Quantum Chem. 20 (2001) 242.
[15] T.C. Ramalho, C.A. Taft, J. Chem. Phys. 123 (2005) 54319–54326.
[16] T.C. Ramalho, R.R. da Silva, J.M. Santos, J.D. Figueroa-Villar, J. Phys. Chem. A 110 (2006) 1031–1040.
[17] J.W. McIver Jr., Acc. Chem. Res. 7 (1994) 72.
[18] S. Bocquet, R.J. Pollard, J.D. Cashion, Phys. Rev. B 46 (1992) 11657.
[19] C.A. dos Santos, A.M.C. Horbe, C.M.O. Barcellos, J.B.M. Cunha, Solid State Commun. 118 (2001) 449–452.
[20] A.L. Morales, C.A. Barrero, F. Jaramillo, C. Arroyave, J.M. Greneche, Hyp. Interact. 148 (2003) 135–144.
[21] U. Schwertmann, U. Gasser, H. Sticher, Geochim. Cosmochim. Acta 53 (1989) 1293–1297.
[22] S. Krehula, S. Music, S. Popovic, J. Alloys Compd. 403 (2005) 368–375.
[23] W. Stiers, U. Schwertmann, Geochim. Cosmochim. Acta 49 (1985) 1909–1911.
[24] L.C.A. Oliveira, J.D. Fabris, R.V.A. Rios, W.N. Mussel, R.M. Lago, Appl. Cat. A: Gen. 259 (2004) 253–259.
[25] L.C.A. Oliveira, J.D. Fabris, K. Sapag, M.C. Guerreiro, M. Gonçalves, M. Pereira, Appl. Cat. A: Gen. 316 (2007) 117–124.
[26] W. Ferraz, L.C.A. Oliveira, R. Dallago, L. Conceição, Catal Commun. 8 (2007) 131–134.
[27] R.C.C. Costa, F. Lelis, L.C.A. Oliveira, J.D. Fabris, J.D. Ardisson, R.R.A. Rios, C.N. Silva, R.M. Lago, Catal. Commun. 4 (2003) 525.
[28] F. Martínez, G. Calleja, J.A. Melero, R. Molina, Appl. Catal. B: Environ. 70 (2007) 452–460.